Aerospace Science and Technology, Volume 94, November 2019, Article number 105387
DOI: 10.1016/j.ast.2019.105387

Low-boom Low-drag Optimization in A Multidisciplinary Design Analysis Optimization Environment

Yicheng Sun*, Howard Smith

Cranfield University, School of Aerospace Transport and Manufacturing, Bedford, MK43 0AL, UK

Abstract: This paper introduces a multidisciplinary design analysis and optimization environment called GENUS. The GENUS aircraft design environment's key features are that it is modular, expandable, flexible, independent, and sustainable. This paper discusses the application of this environment to the design of supersonic business jets (SSBJs). SSBJs are regarded as the pioneers of the next generation of supersonic airliners. Methodologies appropriate to SSBJs are developed in the GENUS environment. The Mach plane cross-sectional area is calculated based on the parametric geometry model. PANAIR is integrated to perform automated aerodynamic analysis. The drag coefficient is corrected by the Harris wave drag calculation and form factor method. The sonic boom intensity is predicted by the wave form parameter method, which is validated by PCBoom. The Cranfield E-5 SSBJ is chosen as a baseline configuration. Low-boom and low-drag optimization are carried out based on this configuration. Through the optimization, the sonic boom intensity is mitigated by 71.36% and the drag decreases by 20.65%.

Keywords: Multidisciplinary design analysis and optimization (MDAO), Supersonic business jet (SSBJ), Sonic boom

Nomenclature

A	ray tube area
$A(x)$	Mach plane cross sectional area
A_e	equivalent area
$A_v(x,\theta)$	longitudinal area distribution
$\bar{c}$	mean aerodynamic chord

*Corresponding author.
E-mail address: Yicheng.sun@cranfield.ac.uk (Y. Sun), Howard.Smith@cranfield.ac.uk (H. Smith)

c_n	speed that a wave propagates normal to itself
C_D	total drag coefficient
$C_{D_{wave}}$	wave drag coefficient
$C_{D_{LV}}$	induced drag coefficient
C_{D_F}	skin friction and form drag coefficient
C_F	skin friction coefficient
C_{L_α}	lift coefficient curve slope
C_{m_α}	moment coefficient curve slope
C_{n_β}	yawing moment derivative due to side slip
C_{l_β}	rolling moment derivative due to side slip
FF	form factor
H_e	energy height
l	overall aircraft length
L/D	lift to drag ratio
$L(x,\theta)$	lift on a spanwise strip per unit chordwise length
M	Mach number
p	overpressure
P_s	specific excess power
r	radius in polar coordinate
S_{ref}	reference area
S_{wet}	wet area
X_{cg}	center of gravity position on x axis
X_{NP}	neutral point on x axis
β	$\sqrt{M^2-1}$
θ	angle between the Y-axis and a projection onto the Y-Z plane of a normal to the Mach plane
ρ	air density
χ	$x-\beta r$

1. Introduction

There has been a renewed, worldwide interest in developing an environmentally friendly, economically viable and technologically feasible supersonic transport aircraft. A historical overview indicates that the supersonic business jet (SSBJ) will be the pioneer for the next generation of supersonic airliners [1, 2]. Mitigation of the sonic boom intensity is vital if the vehicle is to be permitted to operate over land and hence be environmentally friendly. Additionally, improving the aerodynamic efficiency will decrease the fuel consumption and hence be economically viable. Many technical developments have impacts on the aircraft performance. Therefore, a practical multidisciplinary design analysis and optimization (MDAO) environment with proper methods is necessary for SSBJ design space exploration.

In the literature, there are a number of studies for the distinct parts of low-boom low-drag SSBJ conceptual design space exploration in a MDAO environment. Torenbeek [3] designs a Mach 1.6 supersonic business jet concept in a low-fidelity multidisciplinary environment. Laban and Herrmann [4] analyze the architecture of a MDO framework for supersonic transport design but the study lacks a sonic boom prediction tool. Rallabhandi and Mavris [5] study the supersonic business jet concept in an MDAO environment and stress the importance of parametric geometry for wave drag calculations. Mack [6] develops a supersonic business jet concept for low sonic boom design only. Ban et al. [7] explore the design space of a supersonic concept, but their study focuses only on the twin-fuselage biplane configuration. This paper reports further research based on the previous supersonic transport studies [8, 9]. In this paper, we develop an SSBJ design model in an MDAO environment [10] and explore the design space of low-boom and low-drag SSBJ designs through optimization.

This paper is organized as follows: Section 2 gives an overview of the design philosophy and the roadmap of GENUS development. Section 3 describes the function of each module and the appropriate methods for SSBJ modelling. Section 4 introduces a SSBJ case study designed at Cranfield University. Section 5 gives the low-boom and low-drag optimization results. The last section discusses the conclusions.

2. The GENUS Aircraft Design Environment

The widely known aircraft conceptual design theories are Raymer's [11], Howe's [12], Roskam's [13], Stington's [14], Corke's [15] and so on. They provide a multidisciplinary view for the design process, whereas their methods are mainly empirical or simple analytical. In addition to the printed version of methods, there are many computerized

options available range from single-disciplinary codes to multidisciplinary design environments [16-21]. With the computation power increasing, the Euler CFD method is showing great potential in supersonic aircraft designs [22-25].

As it is the aim of the GENUS Aircraft Design environment [10] to provide a multidisciplinary multi-fidelity framework both for designers to use existing, and for researchers to develop new, methods for aerospace vehicle design. The environment is able to synthesize and analyze any aerospace vehicle concept that consists of body components (fuselage, engine pod, external tank, tail boom, etc.) and/or lifting surfaces (wing, horizontal tail, vertical tail, canard, etc.). GENUS provides a good framework for supersonic transport design.

The GENUS environment was envisioned by Professor Howard Smith, head of the Aircraft Design Group. Biologically, genus is positioned above the rank of species and below the rank of family in the hierarchy. For us, the name signifies the connection between the various 'species' of aerospace vehicles (Fig. 1), and the design environment's ability to encompass the design methods for all of them. GENUS has been applied to several projects [26-30].

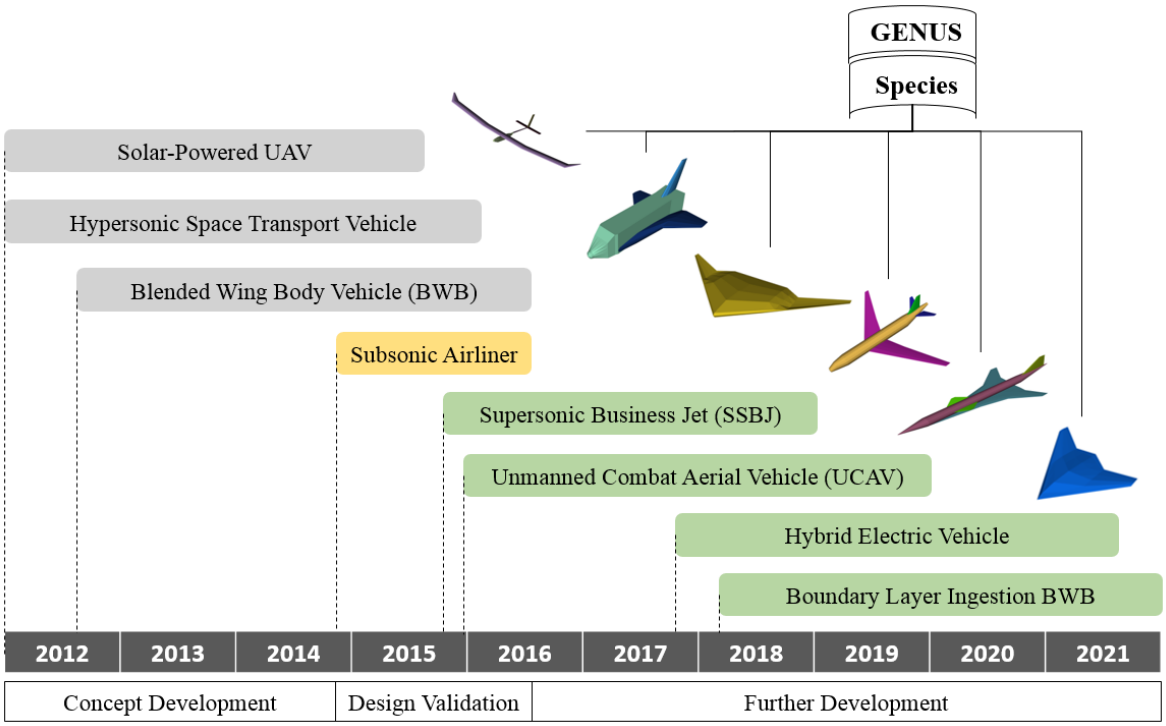

Fig. 1. Roadmap of GENUS development

3. Design Analysis and Optimization Methodologies

The SSBJ model in GENUS includes nine essential modules and a special module, as shown in Fig. 2. The abstract class and subclasses hierarchy of each module is shown in Ref. [8]. Sonic boom prediction is a special module adding to the framework. The modules are linked together tightly, which makes the multidisciplinary design analysis and optimization possible. This section concisely introduces the function and methodologies used in each module.

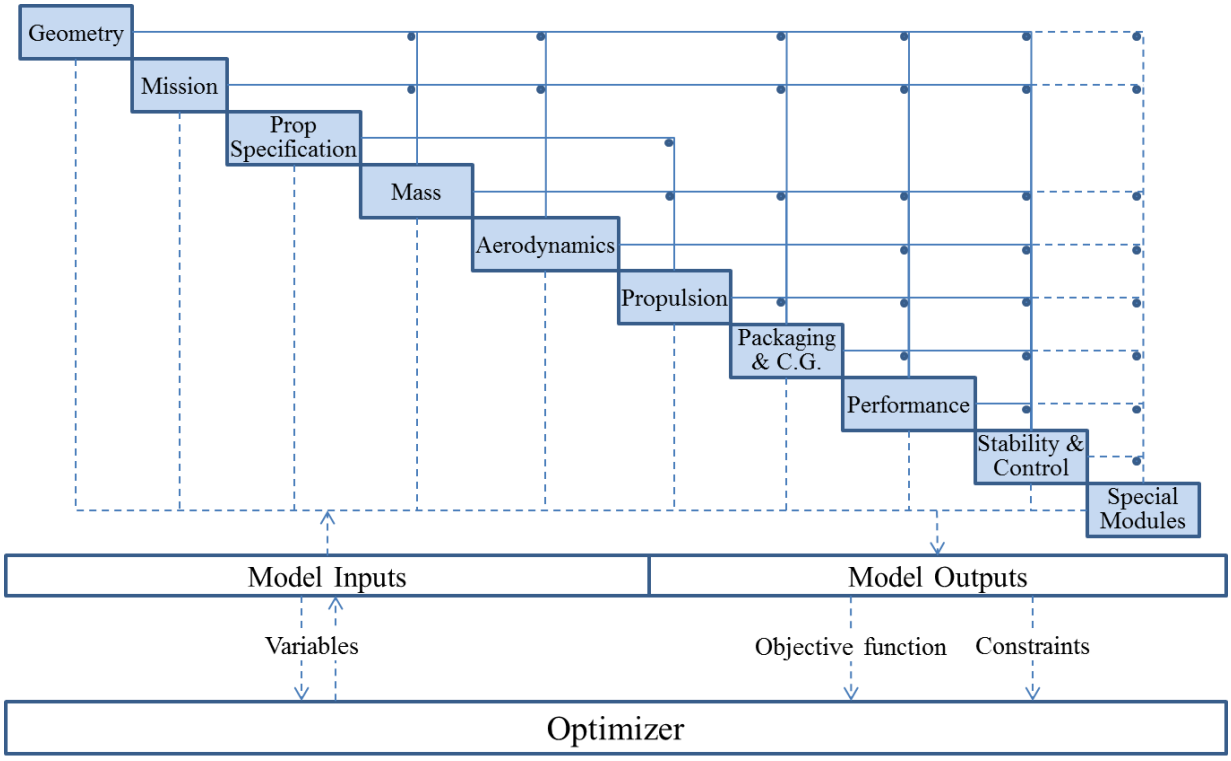

Fig. 2. Modules and data flow of GENUS

3.1. Geometry Generation

The geometry module aims to cover most of the configurations with a generic model. The geometric parts are abstracted into lifting surface and body component arrays. The lifting surface array is then specified as a wing, horizontal tail, vertical tail or canard. The body component array is specified as a fuselage, engine pod, external tank or tail boom. The length of the two arrays depends on the aircraft configuration. A zero-length body component array is applicable to a flying wing type aircraft, whereas a zero-length lifting surface array could represent a space capsule. The inputs for geometry are designed to be intuitive to users. An illustration of the geometry variable definitions can

be found in Ref. [27]. Users can preset input variables' values inside the code so that when running the same configuration, there is no need to input the same value every time.

The geometry generation module is the foundation of the MDAO environment because it is critical to the analysis of the external surface (aerodynamics and sonic boom) and internal (mass breakdown and packaging) components. The geometry is generated by VTK (Visualization Toolkit) [31], which is an open source software for 3D computer graphics.

3.2. Mission Profile

The mission module specifies the flight requirements for a design. These requirements are derived from the market or customer specifications. The mission requirements, shown in Table 1, for SSBJs have been analyzed by the authors in a review paper in Ref. [1]. These values are assumed to be the appropriate initial requirements for environmentally friendly and economically viable SSBJs.

Table 1 Mission requirements for SSBJs

Mission requirement	**Value**
Range	4000 - 4500 nm
Cruise Mach number	1.4 - 2.0
Cruise altitude	<17 km
Seating capacity	8 - 12
Emission	<15 gNO_x/kg fuel
	~1400 g water/kg fuel
Cumulative airport noise	Stage 4-10 dB
Sonic boom intensity	<0.5 psf*

* 1 psf = 47.85 Pa

3.3. Propulsion Specification

The function of the propulsion specification module is to assign requirements regarding the propulsion system of the vehicle. The propulsion specification module specifies the type of engine and fuel to use and the requirements for the propulsion system. There can be a combination of different types of propulsion systems for a hybrid power system.

As with all aspects of supersonic aircraft design, the propulsion system is heavily constrained by numerous requirements. Better fuel efficiency is of high importance to improve the payload fraction and will contribute to a reduction of emissions.

3.4. Propulsion Model

The propulsion module calculates the engine performance at any flight condition. The engine available thrust and corresponding specific fuel consumption (SFC) are stored in two matrices. Users can extract the engine performance at given flight condition by interpolating the Thrust-Mach-Altitude-Throttle matrix and the SFC-Mach-Altitude-Throttle matrix.

The propulsion model for SSBJ design is a modified version of the NASA EngineSim [32]. EngineSim calculates the engine performance based on engine parameters, including the geometry, material properties, flight condition, throttle setting and so on. EngineSim defines the design point in design mode and then evaluates the off-design performance in its test mode. In GENUS, the core of EngineSim is extracted instead of running the applet. Fig. 3 shows the engine performances of a low-bypass turbofan from the EngineSim model and data [11]. The results give the same trends and similar values over the specific ranges.

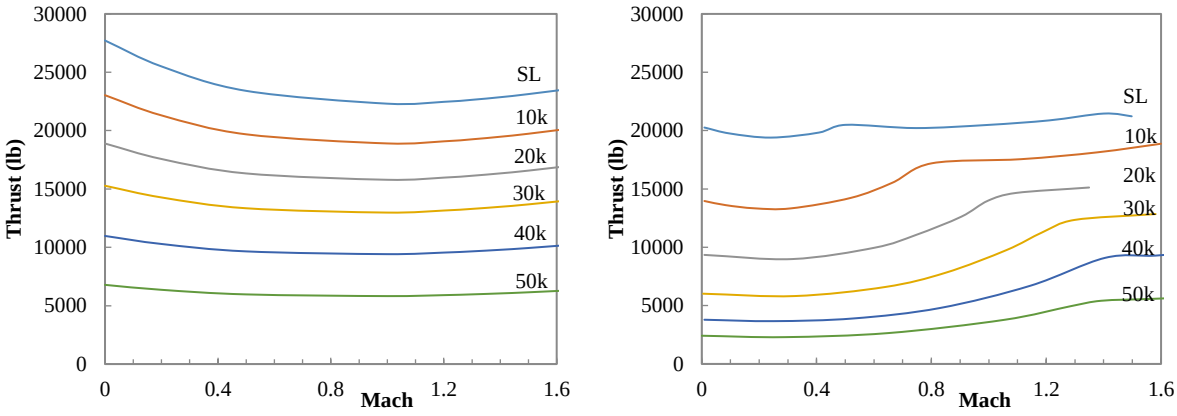

a. Max power thrust from EngineSim model

b. Max power thrust from data

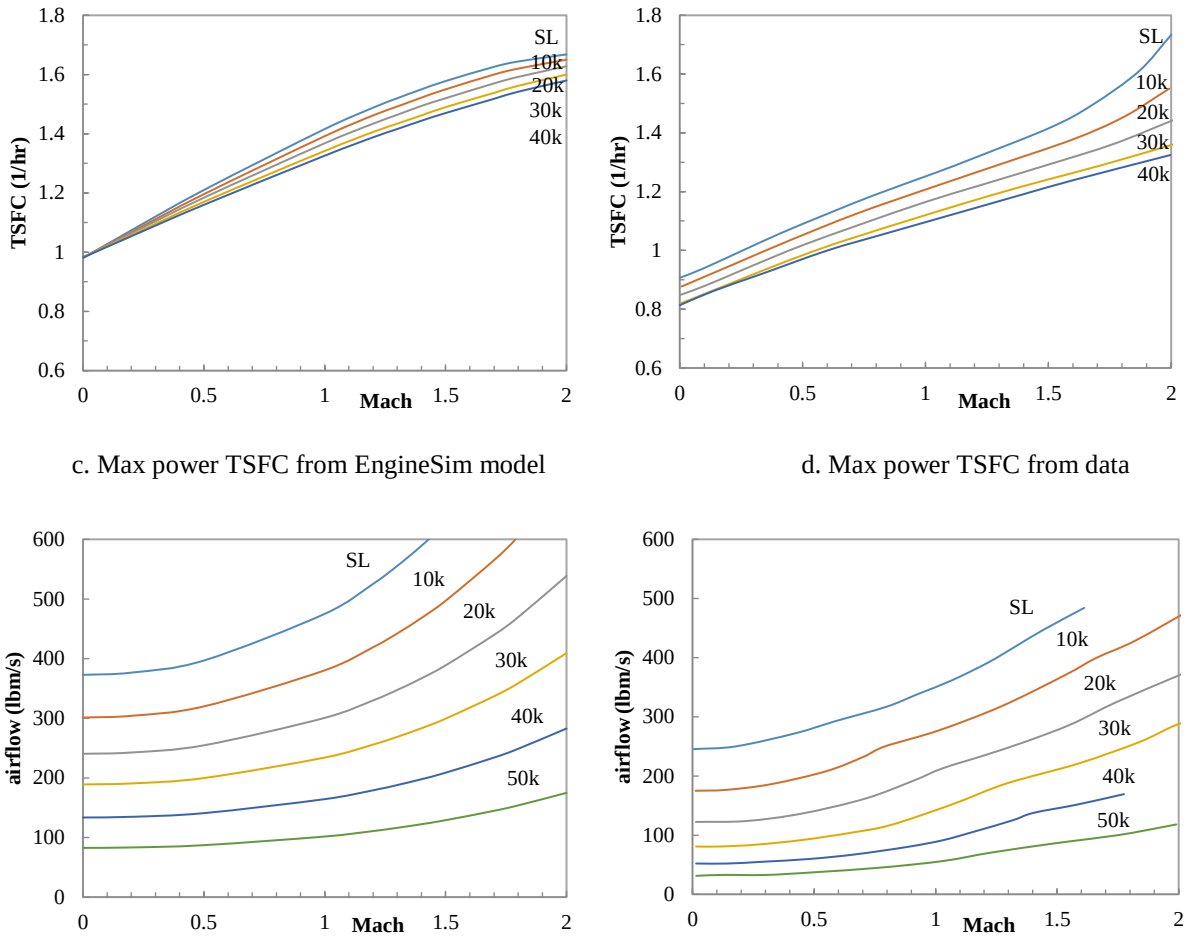

c. Max power TSFC from EngineSim model

d. Max power TSFC from data

e. Engine required airflow from EngineSim model

f. Engine required airflow from data

Fig. 3. Comparison of low-bypass turbofan engine performance

3.5. Mass Breakdown

The mass breakdown module provides a general framework for estimating the mass of various components of an aircraft. Another important function of this module is to decouple the mass components from the packaging module that uses them.

The mass estimation is one of the essential challenges for SSBJ design. It is important to define the start-cruise mass for sonic boom and aerodynamic analyses, which would impact the configuration design in turn. At this stage, only empirical methods are used for SSBJ design. These empirical methods include Howe's mass prediction method [12], Raymer's mass prediction method [11], Torenbeek's method [3], Cranfield in-house mass prediction method, etc. The method chosen is the Cranfield in-house mass prediction method. This method provides not only mass

equations but also the centre of gravity (CG) of each mass component, which is very useful in defining the CG of the whole aircraft. Table 2 gives a comparison between mass calculation results from GENUS and the actual data.

Table 2. MTOM comparison between GENUS calculation and actual data

	Data (kg)	Calculation (kg)	error
Concorde	185000	186568	0.85%
E-5	45454	49052	7.92%
AS-2	54900	50860	-7.36%
S-512	52200	47482	-9.04%

3.6. Packaging

Packaging is a novel and essential module in the GENUS environment. The function of the packaging and CG module is, firstly, to position inner components to detect and avoid interference with other components and the external surface, secondly, to calculate the CG positions for various conditions (with and without fuel or payload). The CG positions are calculated by positioning the mass components from the Mass Breakdown module and they are then used for stability evaluation in Stability and Control.

Packaging is an important aspect of SSBJ design, especially the fuselage volume allocation. On the one hand, the supersonic wave drag reduction tends to an area-ruled fuselage. On the other hand, the passenger cabin and the fuselage fuel tanks require large blocks of volume. An SSBJ cabin is designed to typically accommodate 8-12 passengers. Under the category of comfort, the longer the flight time, the wider the cabin should be. Therefore, the relatively short travel time in an SSBJ should reduce the need for a larger cabin. The packaging layout of the E-5 is shown in Fig. 4.

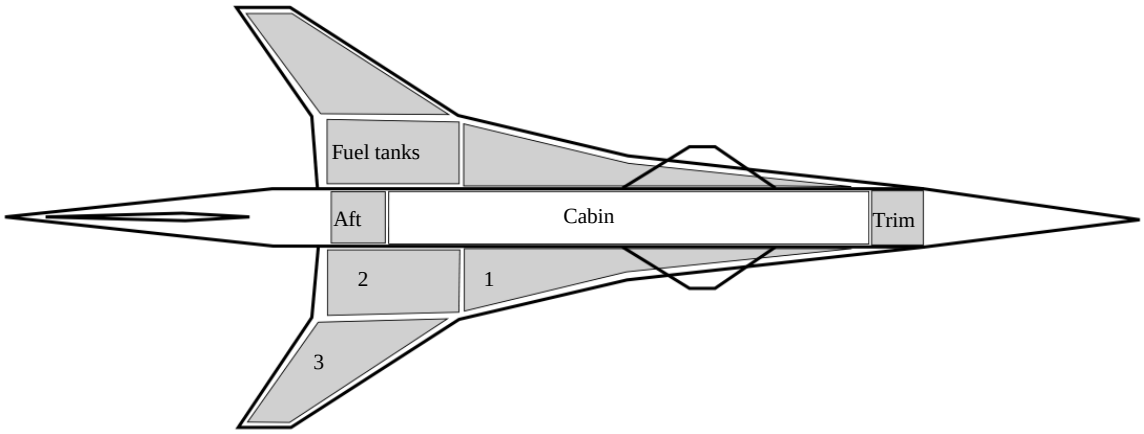

Fig. 4. Fuel tanks packaging

3.7. Aerodynamic Analysis

The aerodynamic analysis module is of vital importance in the aircraft conceptual design process. This module predicts the aerodynamic coefficients using the implemented analysis methods based on the flight conditions and specified geometry. The coefficient matrices are, essentially, a surrogate model, which calculates and stores the coefficients at different Mach numbers and AOA. Users can then extract the requested coefficients at a specific Mach number and AOA by interpolating the matrices.

The aerodynamic analysis tools developed in GENUS include empirical methods from textbooks [11, 12], digital DATCOM [33], vortex lattice method AVL [34], panel method PANAIR [35], and SHABP [36]. The way to automatically use these codes is indicated in Ref. [8]. The capabilities of these aerodynamic analysis codes are listed in Table 3. The A502 solver/PANAIR is a higher order panel method for the computation of the aerodynamic characteristics of different aircraft configurations flying subsonically or supersonically (below Mach 4.0). This code is widely used in SSBJ design [37-39]. The aerodynamic module is capable of using different methods at different Mach numbers. Therefore, these analysis tools can be combined to predict aerodynamic coefficients at subsonic, transonic, supersonic, and hypersonic speeds. Comparisons of Concorde aerodynamic coefficients from the GENUS tools and actual data are shown in Fig. 6.

Table 3. Capabilities of different aerodynamic codes

	Arbitrary Geometry	Subsonic	Transonic	Supersonic	Hypersonic

DDATCOM	×	✓	✓	✓	✓
AVL	×	✓	×	×	×
PANAIR	✓	✓	✓	✓	×
SHABP	✓	×	×	✓	✓

The drag components for supersonic flight consist of zero lift drag, wave drag, and vortex drag, as accumulated in Eq. **(1)**. The lift induced drag is given by PANAIR.

$$C_D = C_{D_F} + C_{D_{wave}} + C_{D_{LV}} \tag{1}$$

The form factor method [40] is modified to calculate the zero-lift skin friction and form drag. The result comes from the contribution of each component, as shown in Eq. **(2)**

$$C_{D_F} = \sum_{j=1}^{N} \frac{FF_j C_{F_j} S_{wet_j}}{S_{ref}} \tag{2}$$

where N is the number of components used to model the configuration.

The wave drag by supersonic area rule [41] is applied for the wave drag calculation, as indicated in Eq. **(3)** and Eq. **(4)**.

$$C_{D_{wave}}(\theta) = -\frac{1}{2\pi}\int_0^l \int_0^l \mathrm{A}''(\theta, x_1)\mathrm{A}''(\theta, x_2) \ln|x_1 - x_2| \, \mathrm{d}x_1 \mathrm{d}x_2 \tag{3}$$

$$C_{D_{wave}} = \frac{1}{2\pi}\int_0^{2\pi} C_{D_{wave}}(\theta) d\theta \tag{4}$$

where θ is the angle between the Y-axis and a projection onto the Y-Z plane of a normal to the Mach plane, as illustrated in Fig. 5.

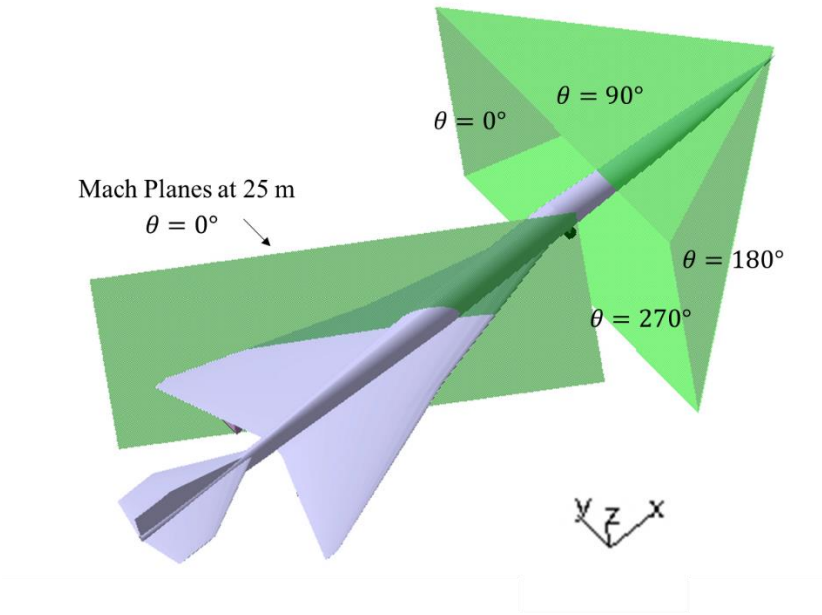

Fig. 5 Illustration of wave drag calculation procedure

The lift and drag coefficients from GENUS (PANAIR and DATCOM) are compared to the Concorde experimental data [42, 43] at Mach 0.95 and Mach 2.0 respectively. Fig. 6a and Fig. 6b indicate that the aerodynamic coefficients from GENUS are close to the results of experimental data, which helps to validate the codes.

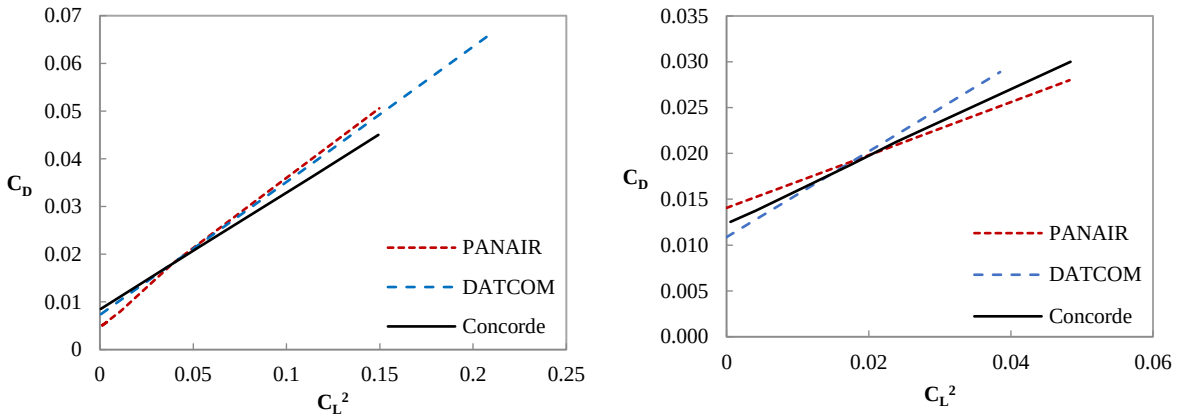

a. Aerodynamic coefficients at Mach 0.95

b. Aerodynamic coefficients at Mach 2.0

Fig. 6. Comparison of Concorde aerodynamic coefficients

3.8. Performance Analysis

The performance module gives the main outcomes of the conceptual design process. This module analyses whether a single instance of the design is capable of fulfilling the mission requirements. Field and point performance are evaluated in this module. The inputs for the module are the user settings for the methods and variables from previous modules. The outputs are the calculated results and error indicators between the results and target values.

In the SSBJ performance analysis module, the whole flight profile consists of several flight points (start of take-off, end of take-off, start of cruise, end of cruise, etc.). The Mach number, altitude, thrust request, aerodynamic coefficients, throttle, C.G. position, etc. at each point are calculated for point performance analysis. The time, distance, fuel consumption, flight path angle, etc. between every two points are calculated for field performance analysis. ESDU Flight path optimization methods [44, 45] are applied for climbing, with the minimum specific excess power (P_s) at each energy height (H_e). Linearly Varying Mach Number Climb/Descent methods are also used for performance trajectory.

3.9. Stability and Control

The stability and control module is designed to evaluate the stability characteristics and trim abilities of the aircraft at various flight conditions. This module does not provide inputs for any module but generates outputs that could be used to drive the optimization process. These outputs are usually error indicators that state whether the aircraft is stable or not in a given flight condition, speed regime and/or the whole mission envelope.

Digital DATCOM [33] is an appropriate tool for stability and control analysis in aircraft conceptual design. The longitudinal and lateral-directional stability characteristics are provided by Digital DATCOM. High-lift devices and control characteristics can be calculated. Trim options are available for subsonic speeds.

The longitudinal stability for an aircraft can be analyzed by comparing the CG position from the packaging and CG module with the aerodynamic centre from the aerodynamic analysis module. The equation for longitudinal static margin (K_n) is as Eq. **(5)**.

$$K_n = \frac{X_{NP} - X_{cg}}{\bar{c}} = -\frac{C_{m_\alpha}}{C_{L_\alpha}} \tag{5}$$

To make the aircraft longitudinally static stable, the static margin K_n has to be positive.

The lateral stability is indicated by C_{n_β} and C_{l_β}. For a lateral stable aircraft, it always holds that: $C_{n_\beta} > 0$ and $C_{l_\beta} < 0$.

A flap or elevator is used for longitudinal control. The trim angle at each flight condition can be calculated by DATCOM.

3.10. Sonic Boom Prediction

The sonic boom is the biggest challenge for SSBJ design; therefore, sonic boom prediction is the essential method for SSBJ design. The sonic boom prediction module demands outputs from the previous modules. There are usually two steps for sonic boom prediction: boom generation and boom propagation. Boom generation specifies the near-field pressure distribution using the volume distribution and lift distribution. Boom propagation is required to propagate the sonic boom to the ground considering the nonlinear turbulence of the atmosphere.

The near-field pressure distribution comes from The Whitham theory [46], as shown in Eq. **(6)**. The F-function depends on the equivalent area A_e given by Eq. **(7)**. A_e consists of A_e due to volume and A_e due to lift as given by Eq. **(8)**. We decompose the F-function into F-function due to volume and F-function due to lift, as indicated in Eq. **(9)**. In this way, we can study their individual effects on sonic boom intensity. The longitudinal lift distribution $L(x,\theta)$ can be calculated by PANAIR. The volume distribution is calculated by the Mach plane equation Eq. **(10)**.

$$\delta p(x) = p_0 \frac{\gamma M^2 F(\chi)}{(2\beta r)^{1/2}} \tag{6}$$

$$F(x,\theta) = \frac{1}{2\pi}\int_0^x \frac{A_e''(\overline{x},\theta)}{\sqrt{x-\overline{\overline{x}}}}\,d\overline{x} \tag{7}$$

$$A_e(x,\theta) = A_v(x,\theta) + \frac{\beta}{2q_\infty}\int_0^x L(x,\theta)dx \tag{8}$$

$$F(x,\theta) = F_{volume}(x,\theta) + F_{lift}(x,\theta) = \frac{1}{2\pi}\int_0^x \frac{A_v''(\overline{x},\theta)}{\sqrt{x-\overline{\overline{x}}}}\,d\overline{x} + \frac{\beta}{4\pi q_\infty}\int_0^x \frac{L'(\overline{x},\theta)}{\sqrt{x-\overline{\overline{x}}}}\,d\overline{x} \tag{9}$$

$$x_i = x - y\cos\theta_0\sqrt{M^2-1} - z\sin\theta_0\sqrt{M^2-1} \tag{10}$$

There are now two methods for boom propagation: the Carlson simplified sonic boom prediction method [47] and the Thomas waveform parameter method [48]. The Thomas waveform parameter method is based on geometrical acoustics [49]. Figure 11 shows a brief schematic of the sonic boom propagation with the waveform parameter method. The results of the sonic boom overpressure from GENUS and PCBoom are shown in Fig. 7.

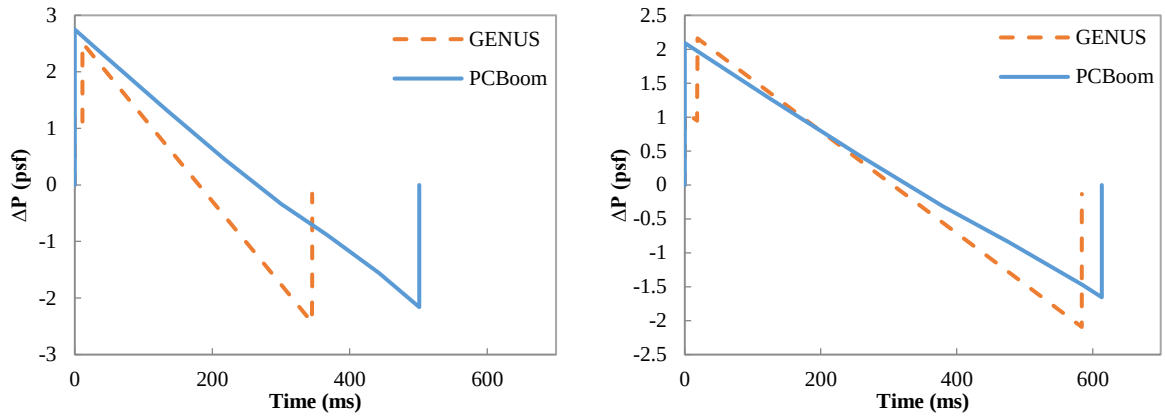

a. Sonic boom overpressure at 40k feet

b. Sonic boom overpressure at 20k feet

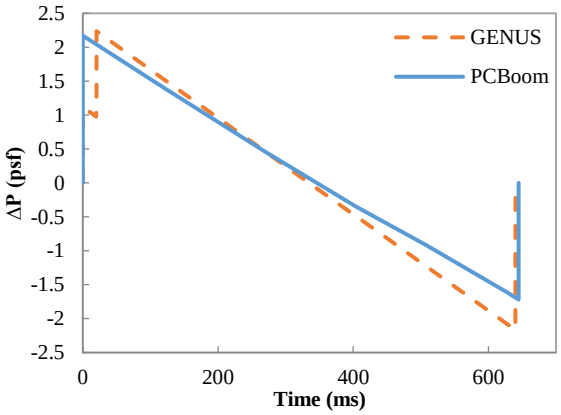

c. Sonic boom overpressure at 10k feet

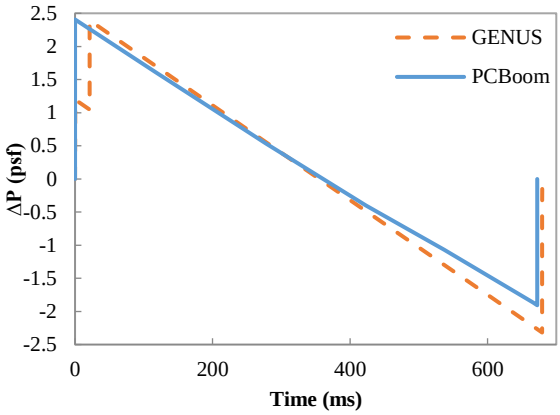

d. Sonic boom overpressure at ground

Fig. 7. Comparison of sonic boom overpressures from GENUS and PCBoom

3.11. Optimization

Optimization is the essential approach for design space exploration. There are a range of optimization methods used in aerospace design. However, there is no one that is suitable for all problems. Thus, it is necessary to have several different optimizers. In GENUS, there are three optimizers: a gradient-based algorithm, a genetic algorithm, and a hybrid algorithm.

4. E-5 SSBJ Baseline Configuration

The design of the E-5 Neutrino Supersonic Business Jet was carried out as a design study by staff and postgraduate students at Cranfield University. Ten academics and some thirty graduate students worked on this design over a period

of seven months. The output of the study comprised the conceptual and preliminary design of the aircraft including its structure and airframe synthesis [50]. The general configuration of E-5 SSBJ is shown in Fig. 8.

The geometry model of the SSBJ has to be fully parametric so that calculations (e.g. Mach plane cross-sectional area calculation) based on the geometry can be accurate. This aircraft features a highly swept wing and a thin aerofoil to decrease supersonic wave drag. The slender fuselage helps to mitigate sonic boom intensity and drag. The canard generates additional vortex lift especially during take-off and landing to facilitate trim.

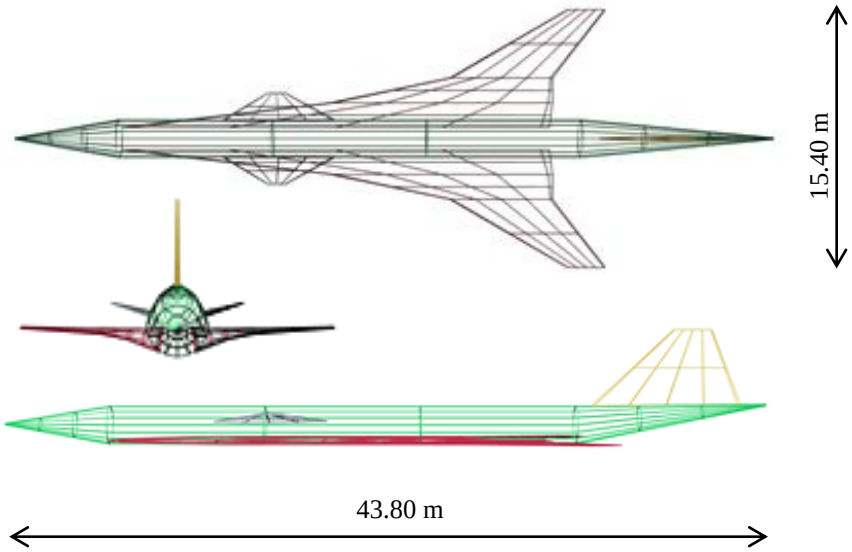

Fig. 8. Three view drawings of the E-5 SSBJ

The mission requirements for the E-5 SSBJ were proposed by Smith [51]. It is noted that an attractive SSBJ design would still need the usual attributes of safety, security, comfort, reliability, performance, and operational flexibility. The requirements are partially used in the GENUS design process as listed in Table 4.

Table 4. Mission requirements for E-5 SSBJ

Requirement	**Value**
Estimated MTOW (kg)	45,454
Take-off distance (m)	3,000
Landing distance (m)	2,000
Cruise altitude (m)	15,000

Cruise Mach	1.8
Target range (km)	8,334
Manoeuvre load factor	2.5
Passenger number	6
Crew number	2

The aerodynamic coefficients are calculated by the panel method PANAIR. The E-5 SSBJ is designed with Hybrid Laminar Flow Control (HLFC) technology, resulting in a laminar flow fraction of 50%-60% on the outer wing [50]. The aerodynamic drag polar with different drag components at cruise speed is plotted in Fig. 9.

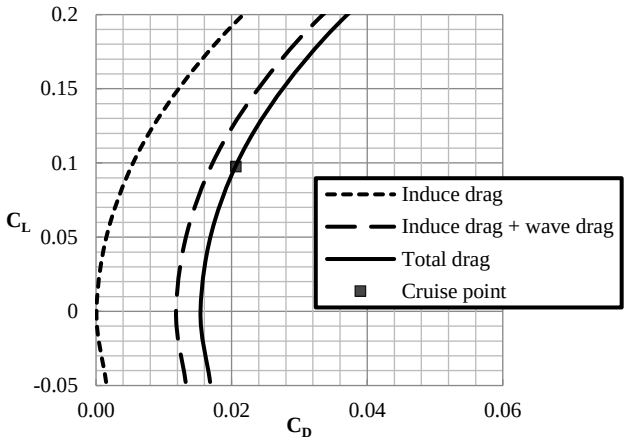

Fig. 9. E-5 SSBJ drag polar during cruise at Mach 1.8

The Mach plane cross-sectional distributions of different components and lift accumulation equivalent area are plotted in Fig. 10a. The equivalent area due to lift accumulation comes from the PANAIR sectional properties. The Mach plane cross-sectional distributions are used for wave drag calculations and sonic boom prediction in the Thomas waveform parameter method. The F-function components, which can help analyze the dominant factor of sonic boom intensity, are plotted in Fig. 10b.

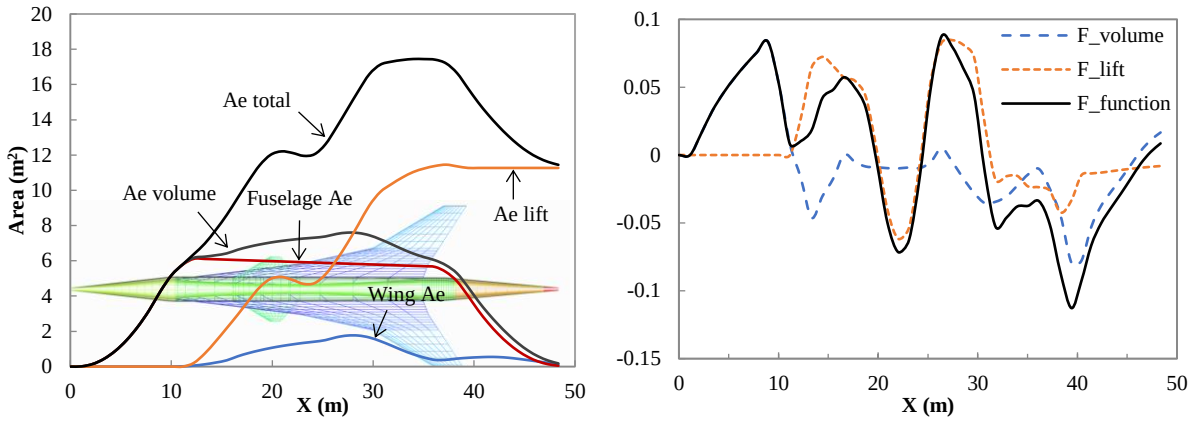

a. Equivalent area distribution b. F-function components

Fig. 10. E-5 SSBJ near-field pressure generation

The near-field and ground sonic boom signatures are shown in Fig. 11. The E-5 SSBJ ground sonic boom maximum overpressure is 2.6 psf. It can be seen that the volume distribution at the front and rear parts have dominating influences on the sonic boom overpressure and underpressure. Therefore, the nose and tail lengths are the main factors for optimization. After the sonic boom intensity decreases to a certain level, the lift distribution will then be the main factors for optimization.

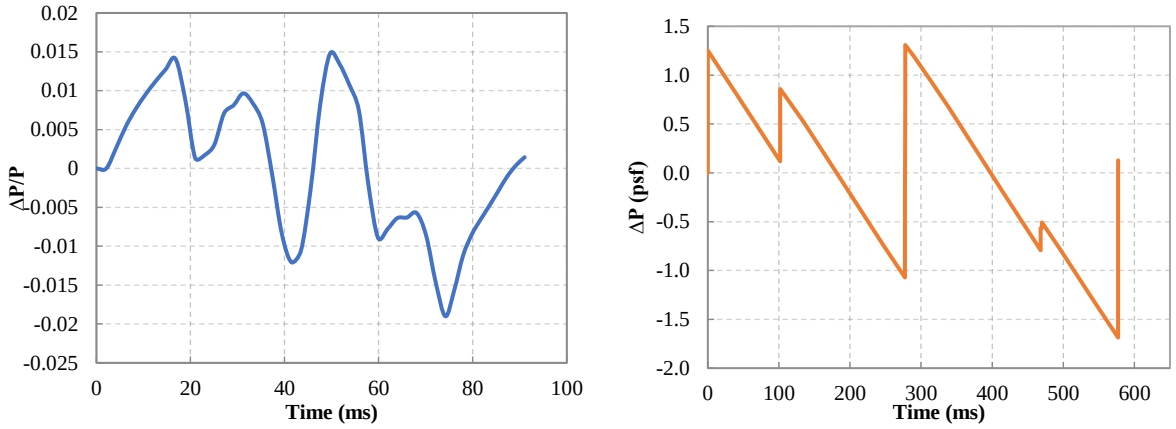

a. Near-field pressure b. Ground pressure

Fig. 11. Near-field and ground pressure of E-5 SSBJ

5. Low-boom Low-drag Geometry Optimization

The E-5 SSBJ was designed, however, without paying too much attention to the mitigation of the sonic boom intensity. In this section, the geometry of the aircraft is optimized to obtain a minimum sonic boom intensity and maximum L/D. The geometry has effects on both the lift distribution and volume distribution. Varying the geometry variables leads to a different near-field pressure distribution, and thus a different sonic boom signature and L/D.

5.1. Low-boom Optimization

For the E-5 SSBJ low-boom optimization, the geometry variables selected for the optimization are nose length, cabin length, tail length, wing section sweeps, wing section dihedrals and wing section spans. The constraints are selected to ensure that the aircraft can fulfil the range requirement, take-off and landing distance requirement, etc. The low-boom optimization setting and results are listed in Table 5.

Table 5. Low-boom Optimization Setting and Results

		Initial	Lower	Upper	Optimization
Objective	Minimize ΔP	2.601 psf	-	-	0.745 psf
Variables	Wing dihedral 1	0.00 deg	-15 deg	10 deg	-8.05 deg
	Wing dihedral 2	0.00 deg	-15 deg	10 deg	-10.06 deg
	Wing dihedral 3	0.00 deg	-15 deg	10 deg	-2.48 deg
	Wing sweep 1	83.30 deg	80 deg	85 deg	80.23 deg
	Wing sweep 2	78.30 deg	70 deg	80 deg	70.84 deg
	Wing sweep 3	60.00 deg	55 deg	65 deg	62.18 deg
	Wing span 1	1.43 m	1.30 m	1.50 m	1.45 m
	Wing span 2	1.45 m	1.30 m	1.50 m	1.46 m
	Wing span 3	3.97 m	3.00 m	4.00 m	3.36 m
	Extra nose length	0.00 m	0.00 m	6.00 m	6.00 m
	Extra tail length	0.00 m	0.00 m	8.00 m	8.00 m
Constraints	MTOM error (=0)	-0.098	-	-	0.001
	Take-off distance error (>0)	0.733	-	-	0.179
	Landing distance error (>0)	0.444	-	-	0.736
	Fuel error (>0)	0.258	-	-	0.362

The near-field pressure and ground signature after optimization are shown in Fig. 12. The sonic boom intensity is 0.745 psf after optimization, which is a big improvement compared to the baseline configuration.

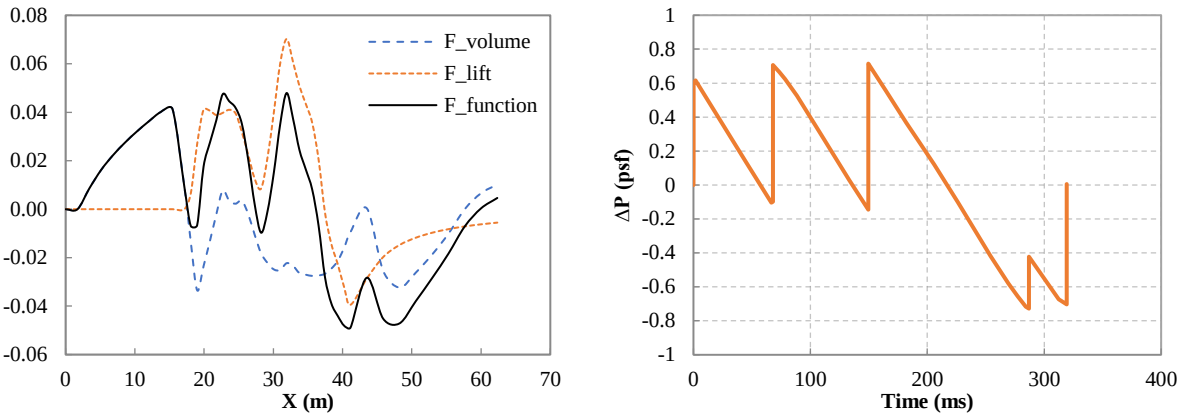

a. Low-boom optimization near-field pressure

b. Low-boom optimization ground pressure

Fig. 12 Near-field and ground pressures for low-boom optimization

Fig. 13 gives the comparisons of the low-boom configuration and the baseline configuration from front view and top view. It can be seen that the nose and tail lengths are increased significantly. The first and second wing kinks have obvious anhedrals. The lift peak is almost the same height as the volume peak (Fig. 12b). If the nose length and tail length are increased further, there will be more scope to reduce the sonic boom intensity.

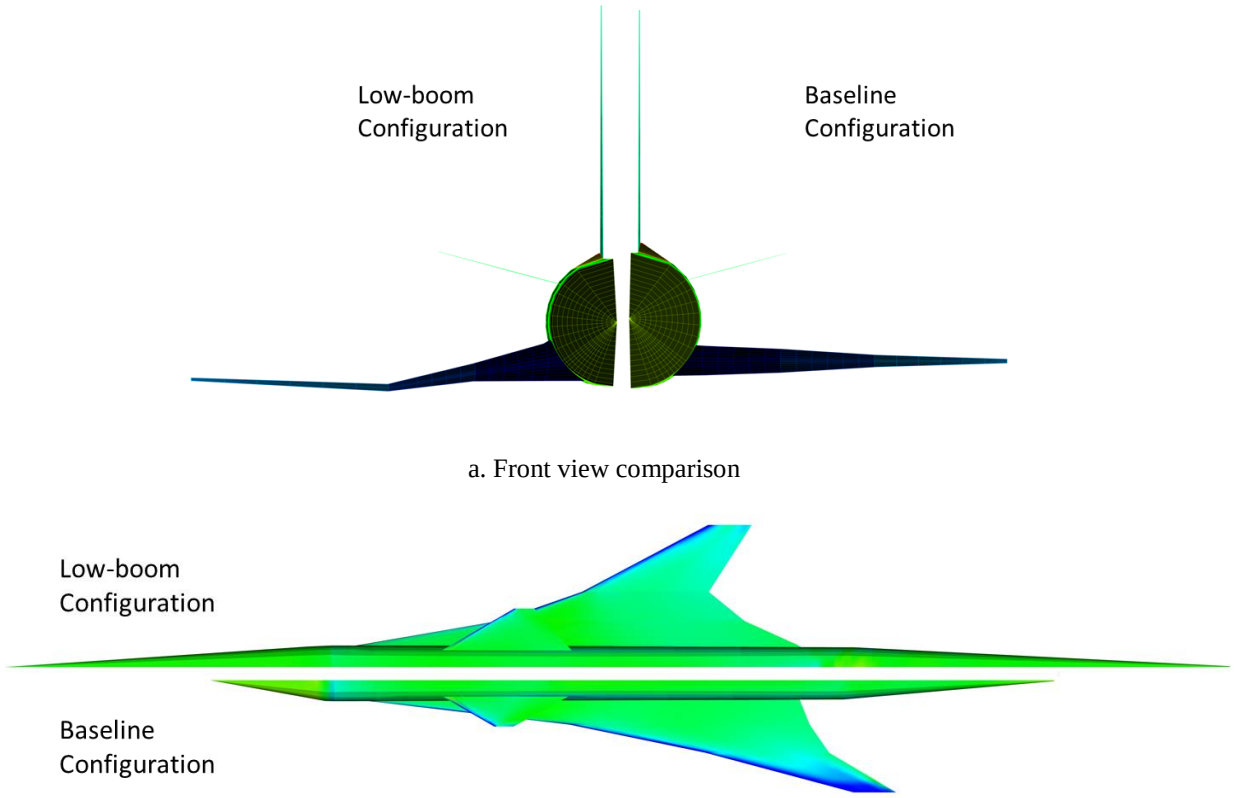

a. Front view comparison

b. Top view comparison

Fig. 13. Geometry comparison before and after low-boom optimization

The convergence history of the objective function ΔP is plotted in Fig. 14. The genetic algorithm converges very quickly. If the objective function is not changed in ten generations, it is regarded as converged. Through Fig. 14b, we can see that the optimization process tends to minimize the sonic boom intensity within a small L/D range.

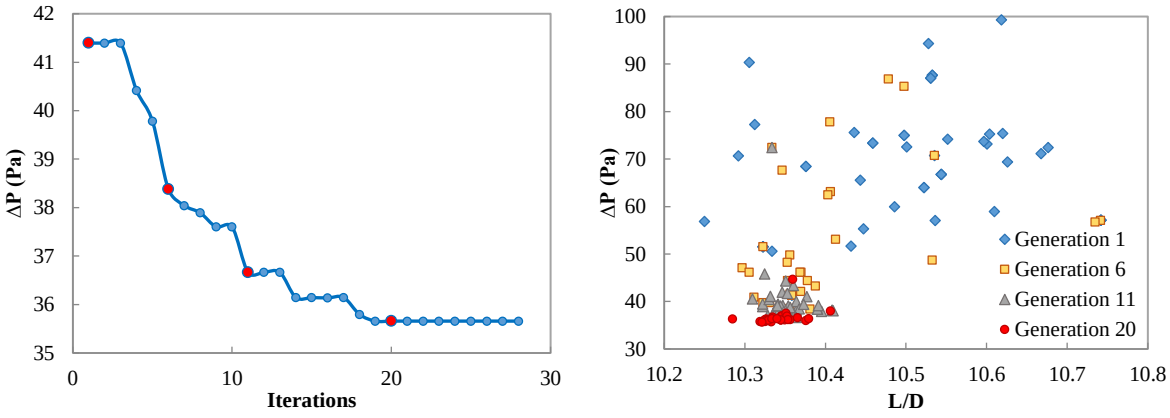

a. Convergence history of objective function ΔP

b. Low-boom optimization generations

Fig. 14. Low-boom optimization process

5.2. Low-drag Optimization with Boom Constraint

For the E-5 SSBJ low-drag optimization, the geometry variables and constraints selected are basically the same as for the low-boom optimization. The extra constraint is the sonic boom intensity, which is constrained to be less than 1.0 psf.

Table 6. Low-drag Optimization Setting and Results

		Initial	Lower	Upper	Optimization
Objective	Maximize L/D	8.96	-	-	10.81
Variables	Wing dihedral 1	0.00 deg	-15 deg	10 deg	-15.00 deg
	Wing dihedral 2	0.00 deg	-15 deg	10 deg	-0.15 deg
	Wing dihedral 3	0.00 deg	-15 deg	10 deg	-2.48 deg
	Wing sweep 1	83.30 deg	80 deg	85 deg	83.31 deg
	Wing sweep 2	78.30 deg	70 deg	80 deg	74.67 deg
	Wing sweep 3	60.00 deg	55 deg	65 deg	59.31 deg
	Wing span 1	1.43 m	1.30 m	1.50 m	1.32 m
	Wing span 2	1.45 m	1.30 m	1.50 m	1.35 m
	Wing span 3	3.97 m	3.00 m	4.00 m	3.79 m
	Extra nose length	0.00 m	0.00 m	6.00 m	6.00 m
	Extra tail length	0.00 m	0.00 m	8.00 m	8.00 m
Constraints	MTOM error (=0)	-0.098	-	-	0.001
	Take-off distance error (>0)	0.733	-	-	0.734
	Landing distance error (>0)	0.444	-	-	0.373
	Fuel error (>0)	0.258	-	-	0.185
	Sonic boom $\Delta P < 1.0$ psf	2.601	-	-	0.9864

The near-field pressure and ground signature are plotted in Fig. 15. After the low-drag optimization, the L/D increases from 8.96 to 10.81. The sonic boom intensity constraint is satisfied with the 1.0 psf requirement.

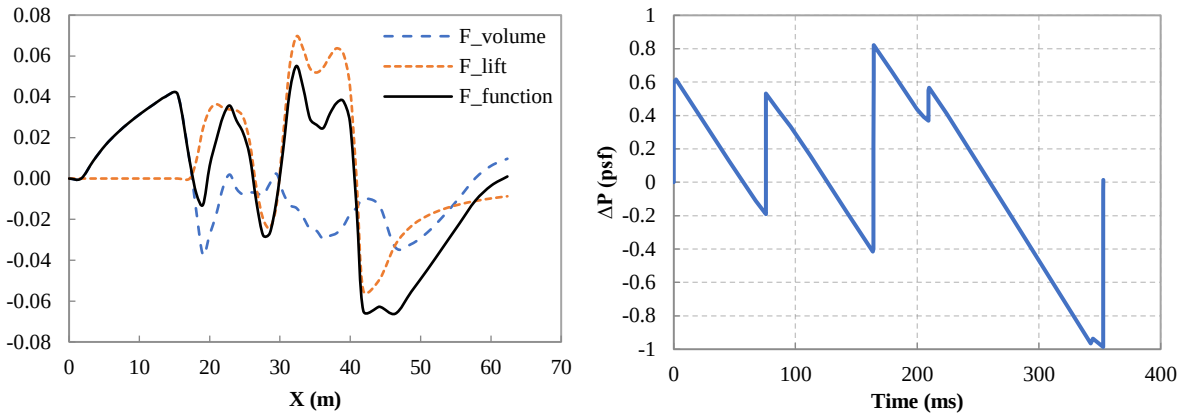

a. Low-drag optimization near-field pressure

b. Low-drag optimization ground pressure

Fig. 15. Near-field and ground pressures for low-drag optimization

As we see from the geometry comparison in Fig. 16, the nose and tail length increase significantly to increase the overall slenderness ratio. The dihedral at the first kink reaches the lower boundary -15 deg, which shows a similar requirement to the low-boom optimization.

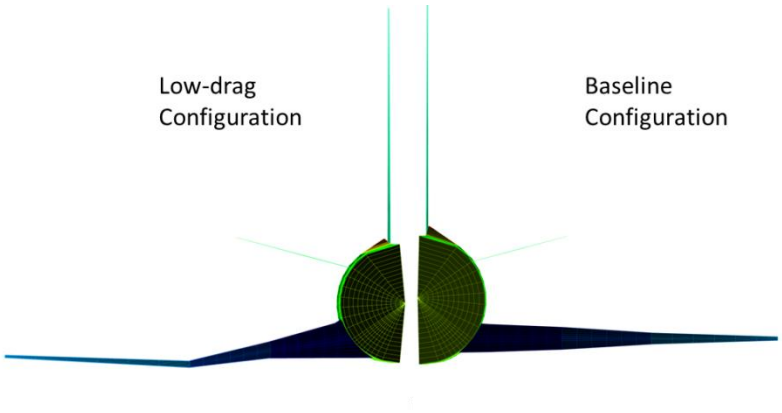

a. Front view comparison

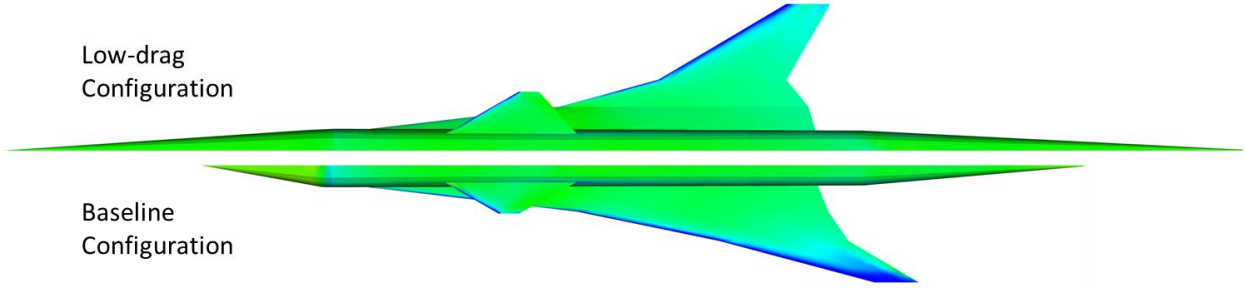

b. Top view comparison

Fig. 16. Geometry comparison of original and low-drag configuration

The low-drag optimization converges more slowly than the low-boom optimization. The sonic boom intensity requirement makes it harder to locate the feasible zone. The optimization process tends to maximize L/D just under the 1.0 psf sonic boom requirement, which is the right bottom corner of Fig. 17b.

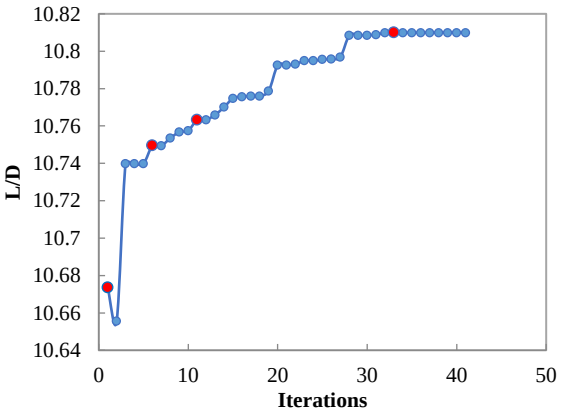

a. Convergence history of objective function L/D

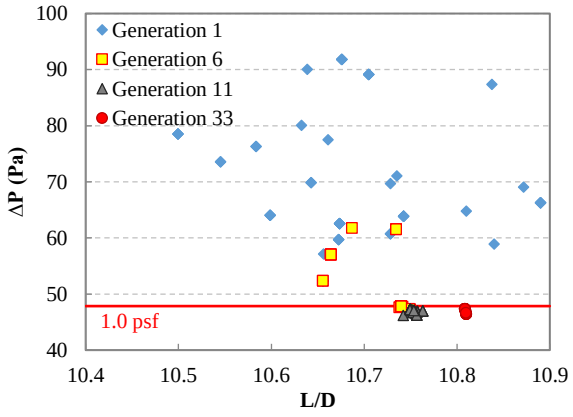

b. Low-drag optimization generations

Fig. 17. Convergence history of objective function L/D

As we can conclude from these two optimization processes, the low-boom design and low-drag design have basically the same requirements for geometry. The nose should be a long conical spike to mitigate the front volume peak. The lift distribution is very sensitive to the wing geometry variables. The tail cone should also have a small volume change rate to mitigate the aft volume peak.

6. Conclusion

In this paper, we have introduced the GENUS aircraft conceptual design environment. GENUS is modular, expandable, flexible, independent, and sustainable. The aim is to support knowledgeable aircraft designers with the overall design architecture and some analysis tools. The GENUS SSBJ model reuses the modules and common design methods from the general framework. It also adds major analysis methods appropriate to SSBJ design. These methods include:

- Mach plane cross-sectional area calculation based on the parametric geometry model
- Automated aerodynamic analysis with PANAIR in both subsonic and supersonic speeds
- Drag coefficient correction with the Harris wave drag calculation and form factor method
- NASA EngineSim integration for engine modelling
- Sonic boom module with the Carlson simplified sonic boom prediction method and the Thomas waveform parameter method

An SSBJ model is built in the GENUS aircraft MDAO environment. The geometry module gives a generic method to model the aircraft. The propulsion, mass breakdown, and aerodynamic analysis modules all show relatively good results compared with actual data. The sonic boom prediction methods give a close signature to NASA PCBoom. The optimization module demonstrates the capability to perform design space exploration. Low-boom and low-drag SSBJ designs can be explored based on this model.

In the case study, the Cranfield University E-5 SSBJ is chosen as the baseline configuration. Through the low-boom optimization, the sonic boom intensity decreases by 71.36%. Through the low-drag optimization, the lift to drag ratio L/D increases by 20.65%. The MDAO environment proves its ability for aircraft design space exploration.

Future work includes analysing the sonic boom and supersonic drag of different configurations and deriving more design ideas for low-boom and low-drag supersonic airliner design.

Conflict of interest statement

We declare that there are no conflicts of interest associated with this publication.

Acknowledgments

The authors would like to thank Dr. David Sziroczak for providing assistance on the integration of the PANAIR code and thank Mr. Eduardo Sepulveda Palacios for the coding work on both PANAIR and EngineSim. Yicheng Sun is supported by the China Scholarship Council (CSC) to pursue his Ph.D. degree in Cranfield University.

References

[1] Y. Sun, H. Smith, Review and Prospect of Supersonic Business Jet Design, PROG AEROSP SCI, 90 (2017) 12-38. https://doi.org/10.1016/j.paerosci.2016.12.003
[2] H. Smith, A Review of Supersonic Business Jet Design Issues, AERONAUT J, 111 (2007) 761-776. https://doi.org/10.1017/S0001924000001883
[3] E. Torenbeek, E. Jesse, M. Laban, Conceptual Design and Analysis of a Mach 1.6 Airliner, in: 10th AIAA/ISSMO Multidisciplinary Analysis and Optimization Conference, 2004, AIAA 2004-4541.
[4] M. Laban, U. Herrmann, Multi-Disciplinary Analysis and Optimisation Applied to Supersonic Aircraft; Part 1: Analysis Tools, in: 48th AIAA/ASME/ASCE/AHS/ASC Structures, Structural Dynamics, and Materials Conference, 2007, AIAA 2007-1857.
[5] S.K. Rallabhandi, D.N. Mavris, Aircraft Geometry Design and Optimization for Sonic Boom Reduction, J AIRCRAFT, 44 (2007) 35-47. https://doi.org/10.2514/1.20456
[6] R.J. Mack, A Supersonic Business-Jet Concept Designed for Low Sonic Boom, NASA/TM-2003-212435, 2003.
[7] N. Ban, W. Yamazaki, K. Kusunose, Low-Boom/Low-Drag Design Optimization of Innovative Supersonic Transport Configuration, J AIRCRAFT, 55 (2017) 1071-1081. https://doi.org/10.2514/1.C034171
[8] Y. Sun, H. Smith, Supersonic Business Jet Conceptual Design in a Multidisciplinary Design Analysis Optimization Environment, in: 2018 AIAA/ASCE/AHS/ASC Structures, Structural Dynamics, and Materials Conference, 2018, AIAA 2018-1651.
[9] Y. Sun, H. Smith, Sonic Boom and Drag Evaluation of Supersonic Jet Concepts, in: 2018 AIAA/CEAS Aeroacoustics Conference, 2018, AIAA 2018-3278.
[10] H. Smith, D. Sziroczák, G.E. Abbe, P. Okonkwo, The GENUS Aircraft Conceptual Design Environment, P I MECH ENG G-J AER, (2018). https://doi.org/10.1177/0954410018788922
[11] D.P. Raymer, Aircraft Design: A Conceptual Approach, Fifth Edition, AIAA, Inc., Reston, VA, 2012.
[12] D. Howe, Aircraft Conceptual Design Synthesis, Professional Engineering Publishing, London and Bury St Edmunds, 2000.
[13] J. Roskam, Airplane Design, DARcorporation, 1985.
[14] D. Stinton, The Design of The Aeroplane, Van Nostrand Reinhold Company, 1983.
[15] T.C. Corke, Design of Aircraft, Prentice Hall Englewood Cliffs, NJ, 2003.
[16] F. Mastroddi, M. Tozzi, V. Capannolo, On the Use of Geometry Design Variables in the MDO Analysis of Wing Structures with Aeroelastic Constraints on Stability and Response, AEROSP SCI TECHNOL, 15 (2011) 196-206. https://doi.org/10.1016/j.ast.2010.11.003
[17] L. Leifsson, A. Ko, W.H. Mason, J.A. Schetz, B. Grossman, R.T. Haftka, Multidisciplinary Design Optimization of Blended-Wing-Body Transport Aircraft with Distributed Propulsion, AEROSP SCI TECHNOL, 25 (2013) 16-28. https://doi.org/10.1016/j.ast.2011.12.004
[18] N.-V. Nguyen, S.-M. Choi, W.-S. Kim, J.-W. Lee, S. Kim, D. Neufeld, Y.-H. Byun, Multidisciplinary Unmanned Combat Air Vehicle System Design Using Multi-fidelity Model, AEROSP SCI TECHNOL, 26 (2013) 200-210. https://doi.org/10.1016/j.ast.2012.04.004

[19] F. Afonso, J. Vale, F. Lau, A. Suleman, Performance Based Multidisciplinary Design Optimization of Morphing Aircraft, AEROSP SCI TECHNOL, 67 (2017) 1-12. https://doi.org/10.1016/j.ast.2017.03.029
[20] C. Alba, A. Elham, B.J. German, L. Veldhuis, A Surrogate-Based Multi-Disciplinary Design Optimization Framework Modeling Wing–Propeller Interaction, AEROSP SCI TECHNOL, 78 (2018) 721-733. https://doi.org/10.1016/j.ast.2018.05.002
[21] P. Panagiotou, S. Fotiadis-Karras, K. Yakinthos, Conceptual Design of a Blended Wing Body MALE UAV, AEROSP SCI TECHNOL, 73 (2018) 32-47. https://doi.org/10.1016/j.ast.2017.11.032
[22] W. Li, E. Shields, K. Geiselhart, Mixed-Fidelity Approach for Design of Low-Boom Supersonic Aircraft, J AIRCRAFT, 48 (2011) 1131-1135. https://doi.org/10.2514/1.c000228
[23] W. Li, S. Rallabhandi, Inverse Design of Low-Boom Supersonic Concepts Using Reversed Equivalent-Area Targets, J AIRCRAFT, 51 (2014) 29-36. https://doi.org/10.2514/1.c031551
[24] I. Ordaz, W. Li, Approximation of Off-Body Sonic-Boom Analysis for Low-Boom Conceptual Design, J AIRCRAFT, 53 (2015) 14-19. https://doi.org/10.2514/1.C033159
[25] W. Li, R. Campbell, K. Geiselhart, E. Shields, S. Nayani, R. Shenoy, Integration of Engine, Plume, and CFD Analyses in Conceptual Design of Low-Boom Supersonic Aircraft, AIAA Paper, 1171 (2009).
[26] G.E. Abbe, Conceptual Design Methodologies for Small Solar Powered Unmanned Aerial Vehicle, School of Aerospace Transport and Manufacturing, Cranfield University, Bedford, UK, 2015.
[27] D. Sziroczak, Conceptual Design Methodologies Appropriate to Hypersonic Space and Global Transportation Systems, School of Aerospace Transport and Manufacturing, Cranfield University, Bedford, UK, 2015.
[28] P.P.C. Okonkwo, Conceptual Design Methodology for Blended Wing Body Aircraft, School of Aerospace Transport and Manufacturing, Cranfield University, Bedford, UK, 2016.
[29] Y. Sun, H. Smith, Turbofan Airliner Conceptual Design in Multidisciplinary Design Analysis Optimization Environment, in: 1st International Conference in Aerospace for Young Scientists, 2016, ICAYS 2016-4029.
[30] E. Sepulveda, H. Smith, D. Sziroczak, Multidisciplinary Analysis of Subsonic Stealth Unmanned Combat Aerial Vehicles, CEAS Aeronautical Journal, (2018) 1-12. https://doi.org/10.1007/s13272-018-0325-0
[31] Visualization Toolkit, http://www.vtk.org/.
[32] NASA, EngineSim Version 1.8a, https://www.grc.nasa.gov/www/k-12/airplane/ngnsim.html.
[33] R. Finck, D. Hoak, USAF stability and control DATCOM, Engineering Documents, 1978.
[34] MIT, Athena Vortex Lattice, http://web.mit.edu/drela/Public/web/avl/.
[35] G.R. Saaris, E. Tinoco, J. Lee, P. Rubbert, A502I User's Manual-PAN AIR Technology Program for Solving Problems of Potential Flow about Arbitrary Configurations, Boeing Document, 1992.
[36] A.E. Gentry, D.N. Smyth, W.R. Oliver, The Mark IV Supersonic-Hypersonic Arbitrary-Body Program, AFFDL-TR-73-159, 1973.
[37] S. Choi, J.J. Alonso, I.M. Kroo, Two-Level Multifidelity Design Optimization Studies for Supersonic Jets, J AIRCRAFT, 46 (2009) 776-790. https://doi.org/10.2514/1.34362
[38] T. Furukawa, Y. Makino, Conceptual Design and Aerodynamic Optimization of Silent Supersonic Aircraft at JAXA, in: 25th AIAA Applied Aerodynamics Conference, 2007, AIAA 2007-4166.
[39] S. Choi, J. Alonso, I. Kroo, M. Wintzer, Multi-fidelity Design Optimization of Low-boom Supersonic Business Jets, in: 10th AIAA/ISSMO Multidisciplinary Analysis and Optimization Conference, 2004, AIAA 2004-4371.
[40] O. Gur, W.H. Mason, J.A. Schetz, Full-Configuration Drag Estimation, J AIRCRAFT, 47 (2010) 1356-1367. https://doi.org/10.2514/1.47557
[41] R.V. Harris, An Analysis and Correlation of Aircraft Wave Drag, NASA TM X-947, 1964.
[42] J. Rech, C.S. Leyman, A Case Study by Aerospatiale and British Aerospace on the Concorde, AIAA Professional Study Series, 1980.
[43] C. Orlebar, The Concorde Story, 6th ed., Osprey Publishing, Oxford, UK, 1997.
[44] ESDU 90012. Energy height method for flight path optimisation, https://www.esdu.com/cgi-bin/ps.pl?sess=cranfield5_1171127173502zrq&t=doc&p=esdu_90012.
[45] ESDU 91016. Energy height method for flight path optimisation, https://www.esdu.com/cgi-bin/ps.pl?sess=cranfield5_1180219123015mfw&t=doc&p=esdu_91016.
[46] G. Whitham, The Flow Pattern of A Supersonic Projectile, Communications on Pure and Applied Mathematics, 5 (1952) 301-348. https://doi.org/10.1002/cpa.3160050305
[47] H.W. Carlson, Simplified Sonic-Boom Prediction, NASA Technical Paper 1122, 1978.
[48] C.L. Thomas, Extrapolation of Sonic Boom Pressure Signatures by the Waveform Parameter Method, NASA TN D-6832, 1972.
[49] M. Berci, L. Vigevano, Sonic Boom Propagation Revisited: A Nonlinear Geometrical Acoustic Model, AEROSP SCI TECHNOL, 23 (2012) 280-295. https://doi.org/10.1016/j.ast.2011.08.003

[50] P. Stocking, E-5 Neutrino Supersonic Business Jet Project Executive Summery, 2005/2006 MSc Aerospace Vehicle Design, 2005.
[51] H. Smith, E-5 Supersonic Business Jet: Design Specification, 2005.

2019-09-20

Low-boom low-drag optimization in a multidisciplinary design analysis optimization environment

Sun, Yicheng

Elsevier

Sun Y and Smith H. (2019) Low-boom low-drag optimization in a multidisciplinary design analysis optimization environment. Aerospace Science and Technology, Volume 94, November 2019, Article number 105387

https://doi.org/10.1016/j.ast.2019.105387